Piconewton Light Force Measurement using Silk Torsion Pendulum

Shivali Sokhi

A dissertation submitted for the partial fulfilment of BS-MS dual degree in Science

Indian Institute of Science Education and Research Mohali
April 2017

Certificate of Examination

This is to certify that the dissertation titled **"Piconewton Light Force Measurement using Silk Torsion Pendulum"** submitted by **Shivali Sokhi** (Reg. No. MS12046) for the partial fulfillment of BS-MS dual degree programme of the Institute, has been examined by the thesis committee duly appointed by the Institute. The committee finds the work done by the candidate satisfactory and recommends that the report be accepted.

Dr. Sanjeev Kumar Dr. Abhishek Chaudhuri Dr. Kamal P. Singh
(Supervisor)

Dated: April, 21, 2017

Declaration

The work presented in this dissertation has been carried out by me under the guidance of Dr. Kamal P. Singh at the Indian Institute of Science Education and Research Mohali.

This work has not been submitted in part or in full for a degree, a diploma, or a fellowship to any other university or institute. Whenever contributions of others are involved, every effort is made to indicate this clearly, with due acknowledgement of collaborative research and discussions. This thesis is a bonafide record of original work done by me and all sources listed within have been detailed in the bibliography.

Shivali Sokhi
(Candidate)

Dated: April, 21, 2017

In my capacity as the supervisor of the candidate's project work, I certify that the above statements by the candidate are true to the best of my knowledge.

Dr. Kamal P. Singh
(Supervisor)

Acknowledgment

I would like to express my sincere gratitude to my supervisor, Dr. Kamal P. Singh, for his guidance, help and consistent support throughout the duration of my masters thesis.

A sincere thanks to Dr. M.S. Sidhu and Sunil Dahiya for their endless assistance and motivation. I also thank all members of the FSL group for making a great working environment and helping me as and when required.

I extend a warm regard to my Master and my family for supporting me in every possible way they could. A special thanks to my friends- Arjit Kant Gupta, Sunil, Jatin, Bindia, Praver, Bharti and IISERM Dance Group for making me enjoy my work.

Special thanks to Dr. Kamal P. Singh for the matlab code for angle detection[Appendix A], Dr. M.S. Sidhu for the LabVIEW program for live tracking of the laser pointer and Dr. Kamal P. Singh and Sumit Mishra for the chamber design details[Appendix B].

Shivali Sokhi

List of Figures

Contents

Chapter 1

Introduction

1.1 Small Force Detection

The measurement of extremely small light forces finds applications in various fields of physics, from optical tweezing of microscopic particles to gravitational experiments with optomechanically coupled measurement systems. Radiation-induced effects are manyfold and so are the physical experiments associated with them[1].

Measurements on real micro/nanosystems at room temperature have led many groups to build specific force machines (weighing balance; for example) and to apply unusual measurement strategies. Effects in this regime include the interplay between Casimir force and Brownian motion and changes in the lever damping induced by electromechanical coupling. Customized force machines based on a Fabry Pérot cavity have been made that are used to investigate light mechanical effects from visible to X ray: bolometric effect, Casimir force and radiation pressure. Also, measurement methods have been devised for spatially rapidly varying forces based on cold damping techniques. Cold damping means here damping through an external feedback loop of the thermal fluctuations.

In force measurement, AFMs can be used to measure the forces between the probe and the sample as a function of their mutual separation. This can be applied to perform force spectroscopy. Depending on the situation, forces that are measured in AFM include mechanical contact force, van der Waals forces, capillary forces, chemical bonding, electrostatic forces, magnetic forces (MFM), Casimir forces, solvation forces etc[2].

Force spectroscopy on the nanoscale is important in studies of fundamental physics, chemistry, and molecular biology and in the design of micro- and nano- opto-mechanical systems[3]. On the subnanometer scale and the micrometer scale, optomechanical manipulation is already an established technique that enables precise force determination. In such systems,

forces are typically measured via the position read-out of a mechanically compliant probe such as a mechanical cantilever or an optically trapped particle[4]. The smallest measurable force is fundamentally limited by the presence of a fluctuating background force exerted on the probe by its thermal environment.
Forces as small as 20 fN have been measured using a method known as photonic force microscopy (PFM), in which the force is determined from the statistics of the thermal motion of the particle.
Other examples include thermoradiative cooling of small oscillators and noise reduction in oscillators due to radiative rigidity cooling[5]. Most of these experiments employ micro-oscillators coupled to an optical cavity that exhibits resonantly enhanced light fields.
Oscillator systems applied for the detection of small forces face a common problem, the presence of fundamental noise associated with the motional degree of freedom[6]. This noise level masks any weak signal acting on the measuring oscillator.

We demonstrate the detection of very small radiation pressure forces at the pico-Newton level without using an optical cavity for enhancing the light field intensity. For this purpose, we employ a torsion pendulum made using a small glass mirror hung via a silk thread with diameter of the order of a few microns. Using a derivative cooling technique, it can be operated at the thermal noise level, giving the desired force resolution sensitivity. The experimental system uses an efficient multi-layer seismic isolation, and provides extremely quiet environmental conditions.

1.2 Torsion Pendulum as a Force Sensor

The torsion pendulum, has been a scientific apparatus for measuring very weak forces ever since the 17^{th} century. It is usually credited to Charles-Augustin de Coulomb, who invented it in 1777, but independently invented by John Michell sometime before 1783[7]. Its most well-known uses were by Coulomb to measure the electrostatic force between charges to establish Coulomb's Law, and by Henry Cavendish in 1798 in the Cavendish experiment[8] to measure the gravitational force between two masses to calculate the density of the Earth, leading later to a value for the gravitational constant.

Ernest Fox Nichols and Gordon Ferrie Hull in 1901 devised a torsional balance setup as a test for the existence of radiation pressure force[9]. The radiant energy of the incident beam was deduced from its heating effect upon a small blackened silver disk. With this apparatus the experimenters were able to obtain an agreement between observed and computed radiation pressures within about 0.6%.

Some recent experiments involving torsion pendulum as a very small force sensor include the opto-mechanical multistability of a macroscopic torsion balance oscillator[10], effect of stochastic resonance where adding noise to nonlinear oscillators can improve the measurement conditions etc[11]. It has recently been used as an automatic apparatus for characterising materials. A sample material is driven into torsional forced oscillation where its motion is sensed, analyzed, and recorded automatically. This mechanical setup is also being used as a test to Newton's Laws of motion at a micometer scale and beyond[12].

Basically, the torsion balance consists of a bar suspended from its middle by a thin fiber. The fiber acts as a very weak torsion spring. If an unknown force is applied at right angles to the ends of the bar, the bar will rotate, twisting the fiber, until it reaches an equilibrium where the twisting force or torque of the fiber balances the applied force. Then the magnitude of the force is proportional to the angle of the bar. The sensitivity of the instrument comes from the weak spring constant of the fiber, so a very weak force causes a large rotation of the bar.

Any twisting of the wire is inevitably associated with mechanical deformation. The wire resists such deformation by developing a restoring torque, τ, which acts to restore the wire to its untwisted state. For relatively small angles of twist, the magnitude of this torque is directly proportional to the twist angle. Hence, we can write

$$\tau = -k\theta,$$

where $k > 0$ is the torque constant of the wire. The above equation is essentially a torsional equivalent to Hooke's law. The rotational equation of motion of the system is written

$$I\ddot{\theta} = \tau,$$

where I is the moment of inertia of the disk (about a perpendicular axis through its centre). The moment of inertia of the wire is assumed to be negligible. Combining the previous two equations, we obtain

$$I\ddot{\theta} = -k\theta.$$

The above Equation is clearly a simple harmonic equation. Hence, we can immediately write the standard solution.

$$\theta = a\cos(\omega t - \phi),$$

$$\omega = \sqrt{\frac{k}{I}}.$$

We conclude that when a torsion pendulum is perturbed from its equilibrium state (i.e., $\theta = 0$), it executes torsional oscillations about this state at a fixed frequency, ω, which depends only on the torque constant of the wire and the moment of inertia of the disk. Note, in particular, that the frequency is independent of the amplitude of the oscillation (provided θ remains small enough).

In the damped case, the torque balance for the torsion pendulum yields the differential equation:

$$I\frac{d^2\theta}{dt^2} + b\frac{d\theta}{dt} + c\theta = 0 \tag{1.1}$$

where I is the moment of inertia of the pendulum, b is the damping coefficient, c is the restoring torque constant, and θ is the angle of rotation.
The solution to the above equation is given by

$$\theta\big(t\big) = \theta_0 e^{-\beta t}\cos(\omega_1 t - \gamma). \tag{1.2}$$

In the experiment to be conducted, the pendulum design is to be independently customised. Hence, we can estimate the torsion constant κ associated with the pendulum. The angular deflection corresponding to a push can be experimentally determined. Hence we can estimate the torque causing the rotation and henceforth the incident force.

1.3 Appropriate Pendulum Suspension

The torsion balance consists of a mass suspended from its middle by a thin fiber. The fiber acts as a very weak torsion spring. If an unknown force is applied at right angles to the ends of the bar, the bar will rotate, twisting the fiber, until it reaches an equilibrium where the twisting force or torque of the fiber balances the applied force. Then the magnitude of the force is proportional to the angle of the bar. The sensitivity of the instrument comes from the weak spring constant of the fiber, so a very weak force causes a large rotation of the bar. So, the choice of the suspending wire is very crucial to the design of the experiment.

The important things to be pondered about are:

- What would be a suitable torsion wire of the lowest possible diameter?

- If the torsion wire is strong enough to hold the suspending mass?
- Can the torsion wire sustain the high vacuum conditions?
- Is the material durable to conduct the experiment for a long enough time?

Chapter 2

Experimental Setup

2.1 Pendulum Design

Biomaterials, having evolved over millions of years, often exceed man-made materials in their properties. Spider silk is one outstanding fibrous biomaterial which consists almost entirely of large proteins. Silk fibers have tensile strengths comparable to steel and some silks are nearly as elastic as rubber on a weight to weight basis. In combining these two properties, silks reveal a toughness that is two to three times that of synthetic fibers like Nylon or Kevlar[13]. They exhibit a unique combination of high tensile strength and extensibility (ductility).

The spider silk diameter ranges from a nm to μm. The relationship between the torsion constant, κ, and the diameter of the wire, d, is given in as

$$\kappa = \frac{\pi G d^4}{32l},$$

where l is the length of the wire and G is the shear modulus for the material of the wire. Therefore, the torsion constant is very sensitively dependent on the diameter of the material. Lesser is the diameter of the suspending thread for a torsion pendulum, greater is the sensitivity. A strong shear modulus, availability of material in extremely low diameters makes is a very effective material to be used as a suspending wire.

We use a bar shaped mirror as the suspending mass for our torsion pendulum. The idea behind using a mirror is that we want to consider solely the effect of radiation pressure force. So, the mass material chosen should be least absorbing and ideally 100% reflecting, so that the absorptive effects do not meddle with the deflection due to radiation pressure.

2.2 Vacuum Techniques

The aim of the experiment is to detect very small radiation pressure forces. To measure forces of the order of piconewton, the pendulum needs to be isolated from all kinds of disturbances other than the pumping source. One such perturbing factor is the air flow surrounding the torsion pendulum. The pendulum is suspended in a UHV compatible vacuum chamber with a maintained pressure of the order of 10^{-7} mbar measured with Newport wide range gauge (WRG). This ultra high vacuum denotes mean free path of air particles of about 10^3 m. This distance is much greater than the dimensions of the vacuum chamber we are using. Hence, at that level of vacuum we can completely neglect the contribution of air particles to the movement of the pendulum and assume that the internal properties of the silk thread are solely responsible for the damping motion of the pendulum.

Vacuum pumps are combined with chambers and operational procedures into a wide variety of vacuum systems. Sometimes more than one pump will be used (in series or in parallel) in a single application. A partial vacuum, or rough vacuum, can be created using a positive displacement pump that transports a gas load from an inlet port to an outlet (exhaust) port. Because of their mechanical limitations, such pumps can only achieve a low vacuum. To achieve a higher vacuum, other techniques must then be used, typically in series (usually following an initial fast pump down with a positive displacement pump). Some examples might be use of an oil sealed rotary vane pump (the most common positive displacement pump) backing a diffusion pump, or a dry scroll pump backing a turbomolecular pump. There are other combinations depending on the level of vacuum being sought.

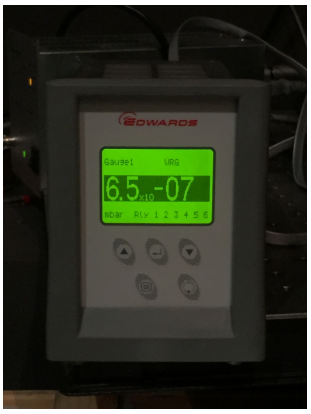

Figure 2.1: Snapshot of the vacuum attained in the UHV chamber.

The following devices were used to attain vacuum of 10^{-7}mbar:

- Pfeffier multistage root pump: This oil free pump is used to get pressure upto 10^{-1} mbar. It pumps out gases from the system. It works as a backing pump for turbo-moleculer pump.
- Pfeffier Turbomolecular pump Hipace80: This high speed pump 15000 rpm is used to achieve around 10^{-5} mbar. It has to be backed up by a roughing pump.
- Agilent Ion pump : This vibration free pumping mechanism system is used under 10^{-5} mbar pressure. This helps in attaining the pressure 10^{-7} mbar without coupling of vibration to the pendulum system.

All three are commercially available.

2.3 Introduction to the Experimental Setup

The experimental setup has been evolving with new improvements being made. In this chapter we present three main stages the experimental setup has been through. The preliminary setup has been addressed as Torsion Pendulum Setup-I. The next stage of the experimental setup with a few modifications has been addressed as Torsion Pendulum Setup-II. The latest setup with multi-layer vibration isolation is addressed as Torsion Pendulum Setup-III.

2.4 Torsion Pendulum Setup-I: Mirror suspended from silk

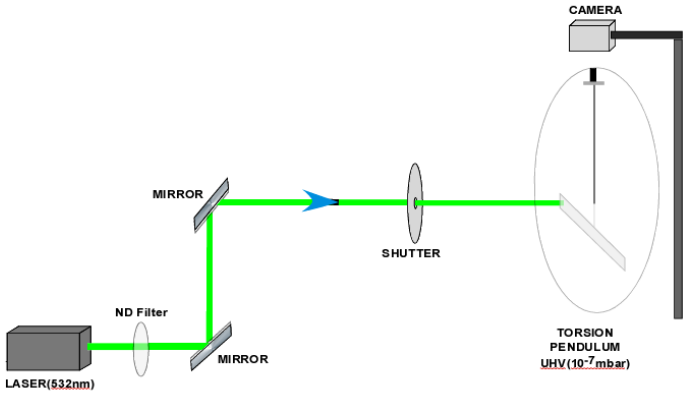

Figure 2.2: Schematic of Torsion Pendulum Setup-I: The 532 nm laser shot is made incident on the mirror and movement is detected using a camera.

- A mirror (aluminum coated coverslip) strip with a thin plastic rod connected to the centre is suspended to a 5-cm-long spider dragline. The whole experiment is settled on a honeycomb core optical table.

- The experiment is conducted at a pressure condition of the order 10^{-6} mbar. The pressure was obtained using a roughing pump followed by a turbo pump and a newly installed ion pump. The turbo and roughing assembly was disconnected after attaining pressure of the order 10^{-5} mbar. The ion pump was working throughout the experiment.

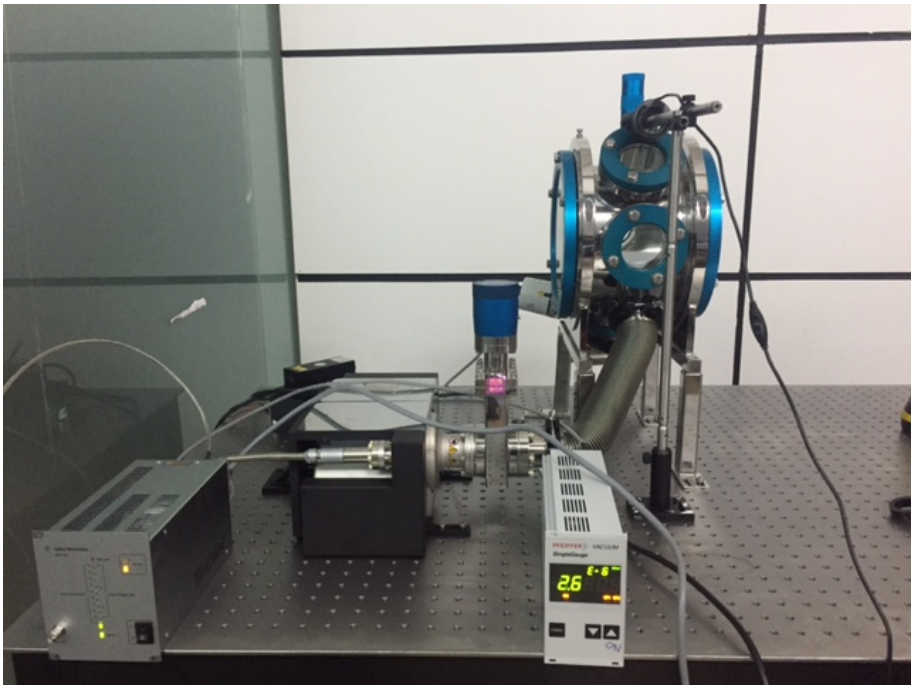

Figure 2.3: Original Image of Torsion Pendulum Setup-I.

- A 532 nm continuous wave laser is made incident on the extreme edge of the mirror bar for precise exposure times using a shutter. The intensity of the light is controlled using an ND Filter.

- The movement of the pendulum was observed and recorded using a web cam. The recorded videos were then analyzed using a Matlab code, which gave a position sensitivity of 2-3 degrees.

2.4.1 Limitations of Torsion Pendulum Setup-I

- The angle detection technique for the pendulum was not good enough. An uncertainty of about 2 degrees always persisted in the measurement.
- There needed to be better isolation from Seismic and acoustic noise from nearby sources.
- The disturbances from the nearby optical instruments like laser and shutter also meddled with the experiment every time a measurement was made.

2.5 Torsion Pendulum Setup-II: Pump-Probe Angle Detection

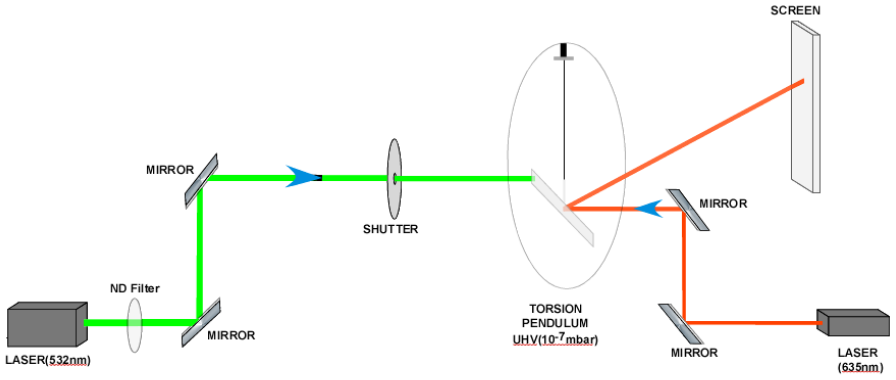

Figure 2.4: Schematic of Torsion Pendulum Setup-II: The 532 nm laser shot is made incident on the mirror and the resultant movement is detected by using a 635 nm probe laser incident on the centre of the mirror.

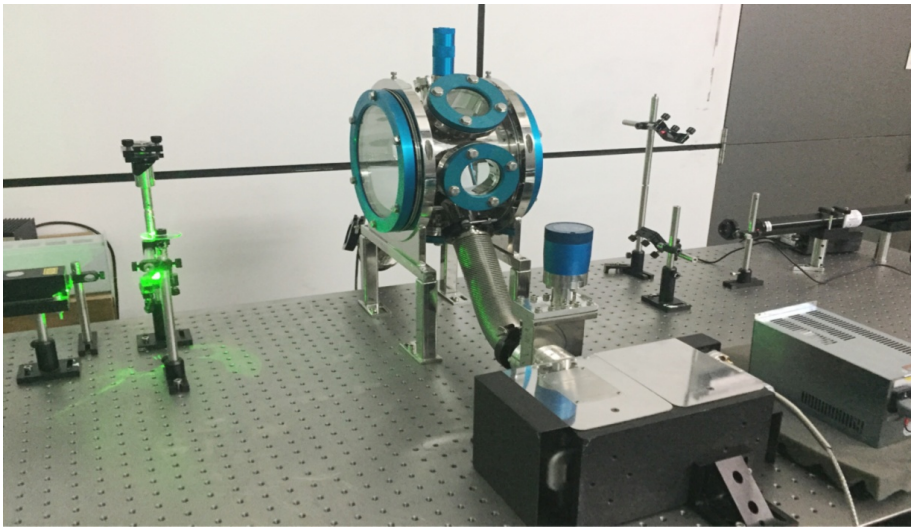

Figure 2.5: Original Image of Torsion Pendulum Setup-II.

2.5.1 Improvisations Made in Torsion Pendulum Setup-I

Pump-Probe type Setup:

- A 635nm continuous wave laser of very low intensity is made incident in the centre of the mirror strip (along the rotational axis). The reflected beam is obtained on a screen. The movement of the reflected point is used to estimate the movement of the torsion pendulum.
- We use a labview program for live tracking of the reflected point. It provides the path tracked by the point along the horizontal and vertical axis. The reflected point is probed on a screen kept 1.25 m away using a camera.

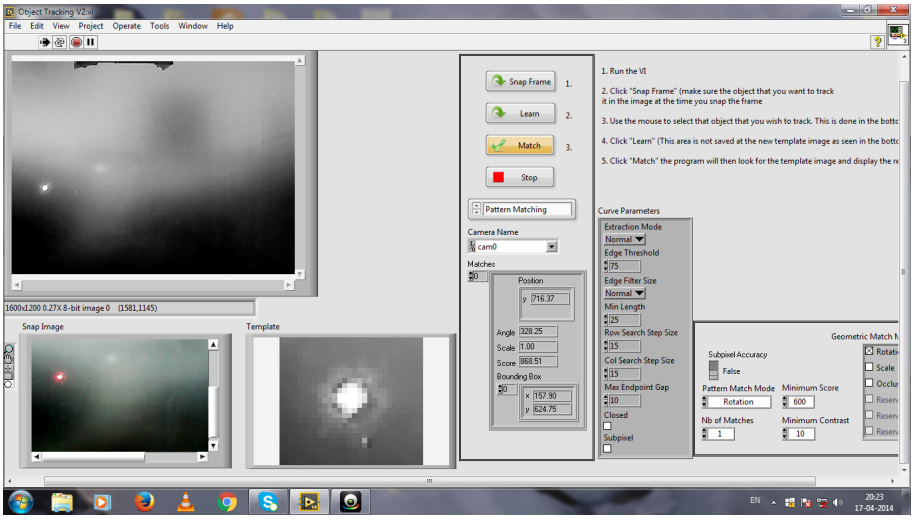

Figure 2.6: Live tracking of a laser pointer using LabVIEW.

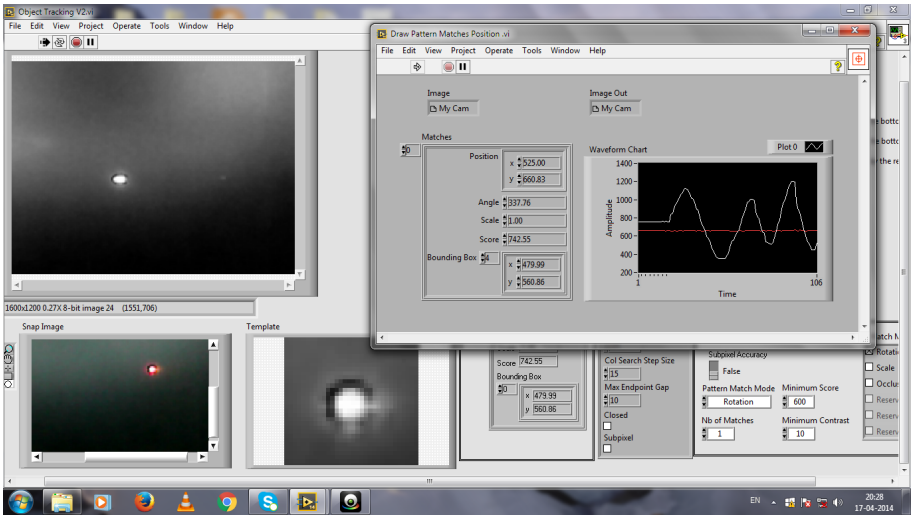

Figure 2.7: The LabVIEW program tracks the movement of the reflected point and plots it in terms of pixel change along x and y axis.

The program snaps a frame from the camera view. An area of interest whose movement is supposed to be detected is selected. We then command it to learn that area and track the displacement along the horizontal and vertical direction.

- The whole experimental setup is set on a Holmarc-AVIS Active Vibration Isolation System.

2.5.2 Limitations of Torsion Pendulum Setup-II

- There was a fundamental noise associated with this configuration. Probable sources are ground vibrations, acoustic noise, thermal noise and disturbance from the nearby optical instruments.
- The table used was faulty. The active control strategy they used was coupling the ground vibrations to the experimental setup.
- The pendulum suspension was not found to be tight enough. Also, the manual rotation suspension imparted a huge disturbance and change to the pendulum whenever even a slight movement was made.

2.5.3 Improvement Possibilities

- Effective Vibration Isolation.
- Designing a vibration free stable suspension for the pendulum.
- Design a pendulum with lower moment of inertia for the detection of very small changes.

2.6 Torsion Pendulum Setup-III-Multi Layer Vibration Isolation

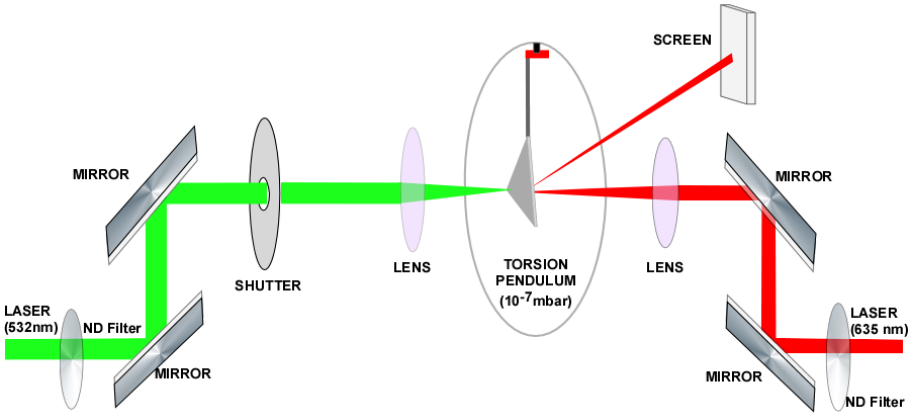

Figure 2.8: Schematic of Torsion Pendulum Setup-III: The 532 nm laser shot is focused on a triangular mirror and the resultant movement is detected by using a 635 nm probe laser focused at the centre of the mirror.

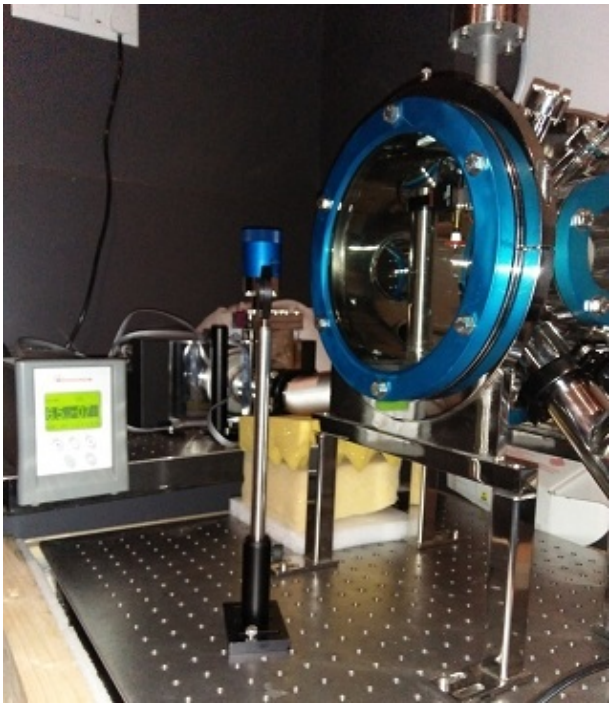

Figure 2.9: Original Image of Torsion Pendulum Setup-III.

2.6.1 Improvisations Made in Torsion Pendulum Setup-II:

Reducing the Moment Of Inertia:

In order to decrease the moment of inertia associated with the pendulum, a small triangular piece of mirror is taken as the subject. It has a relatively lower mass and smaller distance between the incident force and rotational axis. Also, lower the diameter of the suspending silk thread more is the sensitivity; as k is proportional to d^4.

Isolating the Vacuum Chamber:

We isolate the chamber housing the pendulum from all the surrounding optical components as well as the pump and probe system. The ion pump is also placed on a separate optical table. The only connection is the anti-vibration flexible bellow.

Multi-Layer Siesmic Isolation:

The vacuum chamber housing the pendulum is placed on multiple layers of vibration dampener materials. The lowermost layer is a mat of silicon rubber dampener mats. We place a wooden box over the silicon mats and the box is filled with dampener silica sand. An optical breadboard is then placed on 5-inch thick layer of sand and the vacuum chamber is then fixed on it[14].

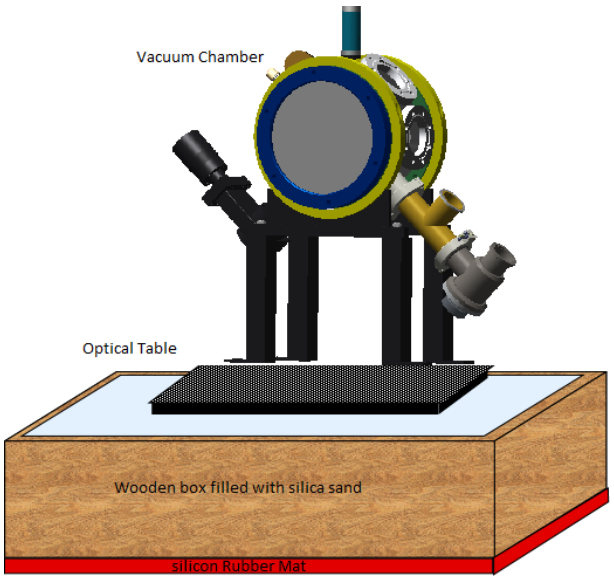

Figure 2.10: Multi-layer vibration isolation using a silicon rubber mat, silica sand filled wooden box and an optical table.

Acoustic Isolation:

The whole experimental setup is placed in an acoustically isolated room and the controls are adjusted in such a way that during an entire measurement there is no walking or seismic disturbance in principal.

Suspension Design:

A circular post was fixed inside the vacuum chamber and a picomotor was attached to it. Picomotor actuators:

- These vacuum compatible Newport picomotor actuators are used to make fine angular displacement of the suspended pendulum so that its plane is nearly perpendicular to the laser beam and the reflection is obtained in the desirable space.
- It has less than 30 nm linear resolution and its vacuum compatibility made it a valuable tool of mounting the suspended silk pendulum.
- At every connection point, small pieces of dampener rubber were inserted so as to dampen all the vibrations associated with the suspension. The rotating head of the picomotor was tightly wrapped with Teflon and a silicon disc was inserted onto it. Torsion pendulums using silk as the suspension thread were fixed on that disc.
- That disc could be very slowly rotated by small amounts so as to change the orientation of the pendulum according to the available reflection space.

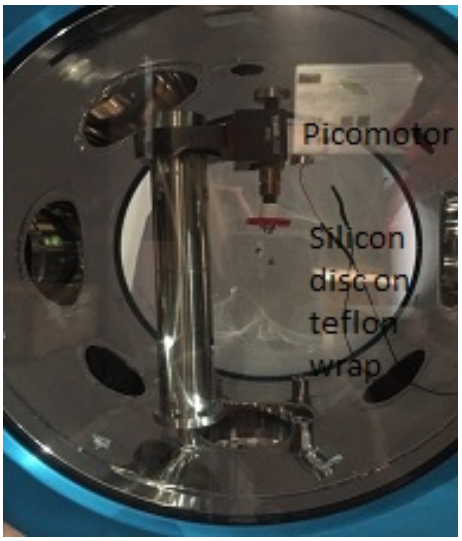

Figure 2.11: Multi-layer Isolation Pendulum Suspension embedded with silicon rubber at every contact point.

Focusing the Laser:

As the mirror used to make the pendulum was of very small dimensions, we had to focus the pump as well as the probe laser beams. Plano-convex lenses were used to focus the laser beams at desirable positions on the triangular mirror.

Chapter 3

Observations and Results

3.1 Torsion Pendulum Dynamics using Setup-II

3.1.1 Pendulum Details

- Length of plastic connection on mirror: 1.3 cm
- Length of thread: 6 cm
- Diameter of thread: 5.7 μm

Figure 3.1: Torsion Pendulum made using a silk thread as the suspending thread.

3.1.2 Varying Exposure time

The experiment was started as a test of the suitable exposure time. A respectable power of 6 mW was taken as the test power because we wished to detect powers lower than this. At a fixed incident power of 6 mW, the change in horizontal motion of the reflected point is noted. Vertical motion of the reflected point was not accounted for. It was assumed that different modes of vibration are not coupled and are independent. We wanted to check the pattern of maximum angular deflection which a laser shot can produce in a torsion pendulum.

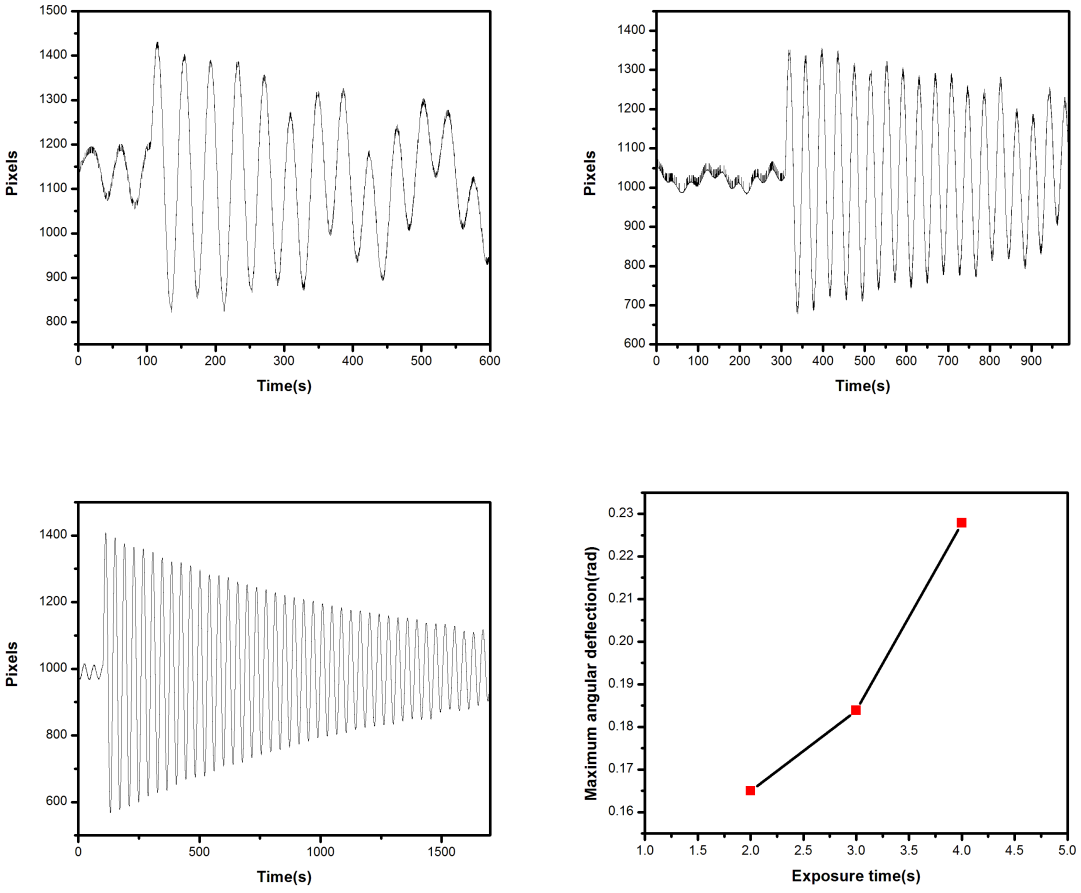

Figure 3.2: The plots show the movement of the reflected point along the horizontal axis when laser light of incident power 6 mW is exposed for 2, 3 and 4 seconds respectively. The last plot shows the maximum angular deflection produced by 6 mW power for different exposure time.

Here the area of screen captured by the camera is divided into a matrix of 1600 x 1200. According to the then set camera,

- 1 pixel = 0.0275 cm
- Distance between screen and pendulum(D) = 320 cm
- $\theta = \frac{Pixelchange}{D}$

We select an exposure time of 2 seconds for performing subsequent experiments and see the nature of change in angular deflection with changing power.

3.1.3 Varying Incident Power

We shine a laser beam onto the mirror for a fixed exposure time of 2 s and see the change in the pendulum position.The aim is to detect as low a force as possible with a signal that is detectable beyond the noise level as whenever we try to make an accurate measurement we discover that the quantities we are observing appear to fluctuate randomly by some amount. This limits our ability to make quick, accurate measurements. So, starting from an incident power of 10 mW and going down the scale, the lowest power corresponding to which a change can be detected is 2 mW using the Torsion Pendulum Setup-II.

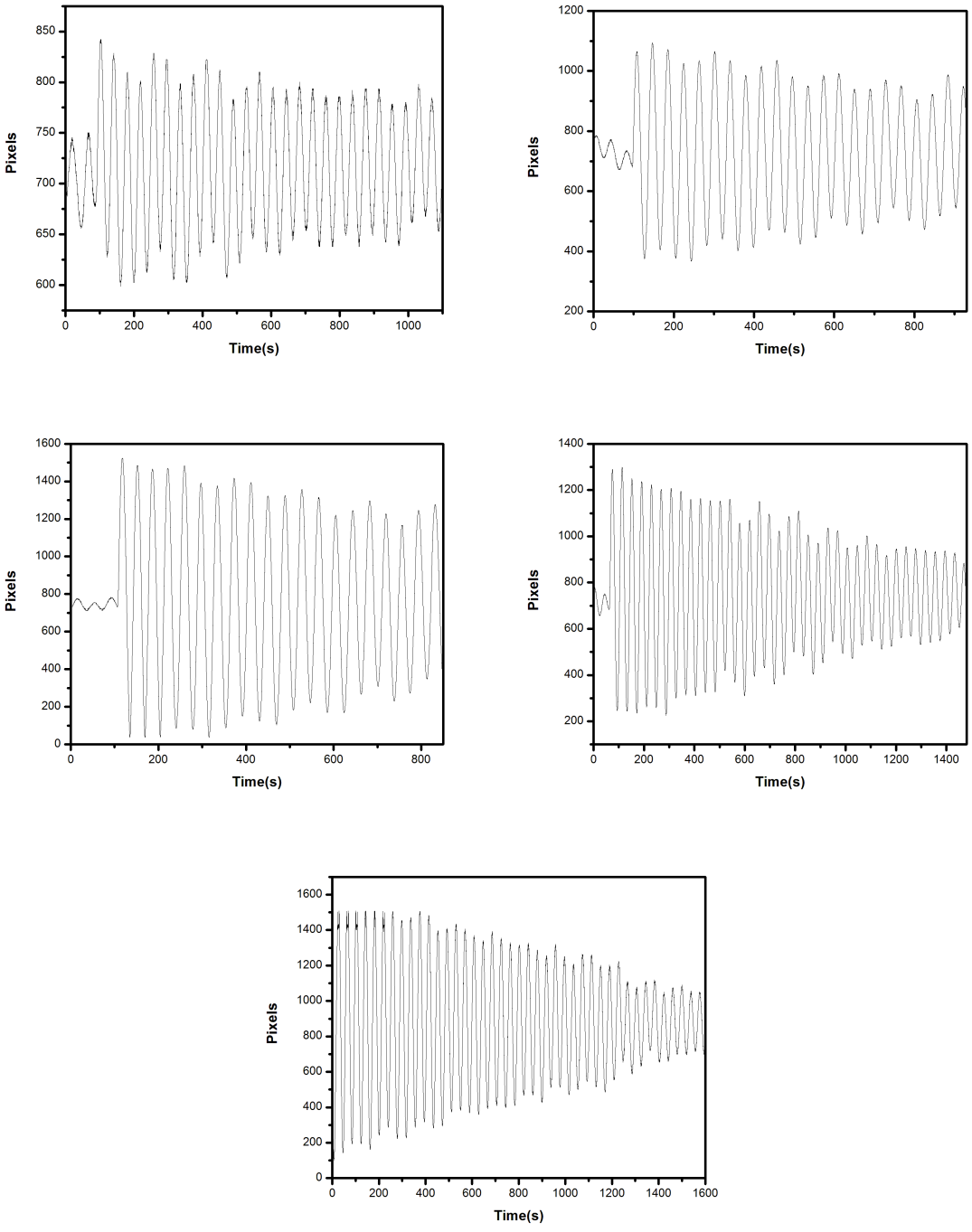

Figure 3.3: The plots show the movement of the reflected point along the horizontal axis on a 2 s exposure of laser light of incident power 2, 4, 6, 8 and 10 mW respectively.

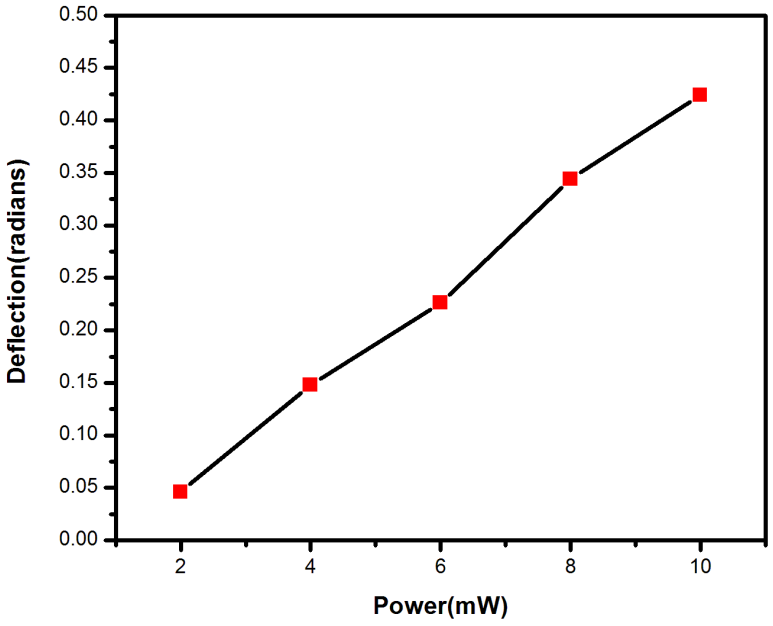

Figure 3.4: Maximum angular deflection produced by laser shots with varying incident power for a fixed exposure time of 2 s.

An account of maximum angular deflection which different laser powers could produce is made. Using the pulse-probe detection technique, The angular precision is of the order of miliradian. We obtained a signal corresponding to the minimum incident power of 2 mW. Assuming the mirror to be perfectly reflecting, the minimum force detected is as follows

$$F = \frac{2P}{c} = 13.3 \times 10^{-12} N.$$

3.2 Noise Analysis

In experimental sciences, noise can refer to any random fluctuations of data that hinders perception of an expected signal. Whenever we try to make accurate measurements we discover that the quantities we are observing appear to fluctuate randomly by a small amounts. This limits our ability to make quick, accurate measurements and ensures that the amount of information we can collect or communicate is always finite. These random fluctuations are called Noise. A common question when designing or using an experimental

systems is, 'Can we do any better?' In some cases it's possible to improve a system by choosing a better design or using it in a different way. In other cases we're up against fundamental limits set by unavoidable noise effects. To decide whether it is worth trying to build a better system we need to understand how noise arises and behaves. Here we try to analyse the noise pattern which always persists in our experiment when the surroundings are supposedly quiet.

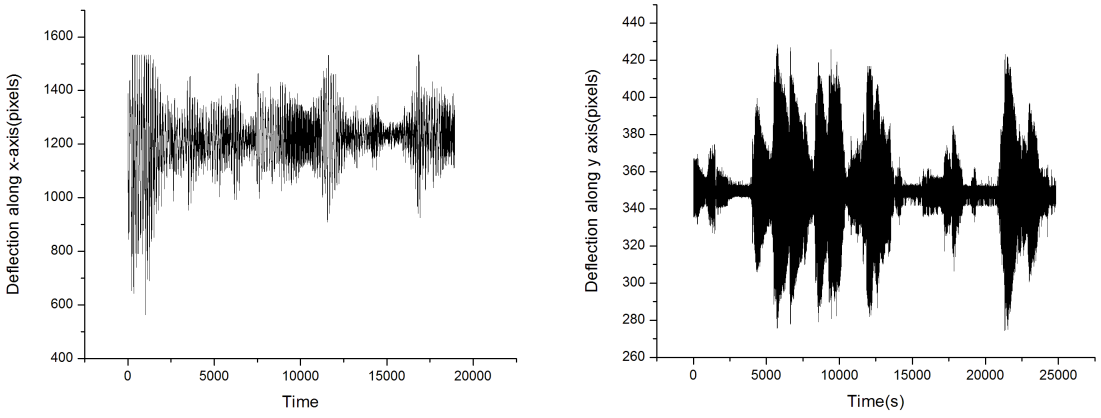

Figure 3.5: x and y deflection of the reflected probe laser point with supposedly no external perturbation.

The movement of the reflected point using the probe is examined over a long period of time without any external perturbation. We perform a fourier transform of the acquired data to see which are the pronounced frequencies causing the disturbance. We then thy to detect and eliminate the sources of distance of nearly that frequency. In addition to investigating potential sources of noise, our hope was to create a new experimental design with relatively lower noise levels and capable of detecting even lower powers.

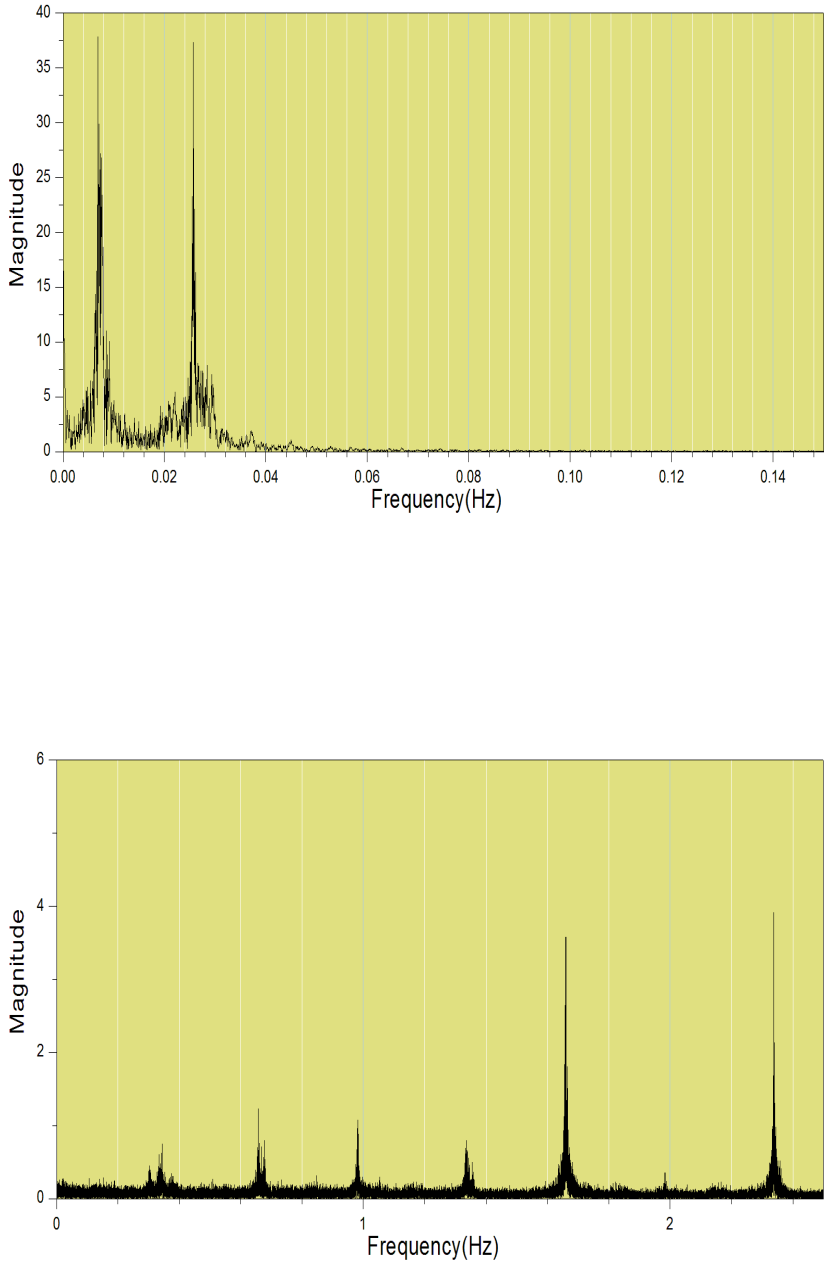

Figure 3.6: On taking FFT of the deflection along x and y axis, magnitude vs frequency graphs of the x and y deflection.

3.3 Torsion Pendulum Dynamics using Setup-III

3.3.1 Pendulum Details:

- Length of suspending thread: 3 cm
- Length of base of triangular mirror(a): 0.3424 cm
- Height of triangular mirror(b): 0.29 cm
- Mass density of mirror material: 34.84 mg/cm^2
- Area Moment of inertia about centroidal axis:

$$I = \frac{ab^3}{36} = 2.3196\ mm^4$$

- Mass moment of ineria = Mass density×Area moment =$8.08\times10^{-13}\ kgm^2$
- Time Period = 7 s
- Using

$$\kappa = \frac{4\pi^2 I}{T^2}.$$

$\kappa = 6.503 \times 10^{-13}\ kgm^2s^{-2}$

3.3.2 Varying Exposure Time

In a setup embedded with multi-layer vibration isolation, we subjected the triangular pendulum to laser shots of powers varying from 10 mW to 0.1 mW. The pulse and probe beams were focused on the small mirror and the horizontal movement of the reflected probe beam (corresponding to torsion oscillations) is recorded.

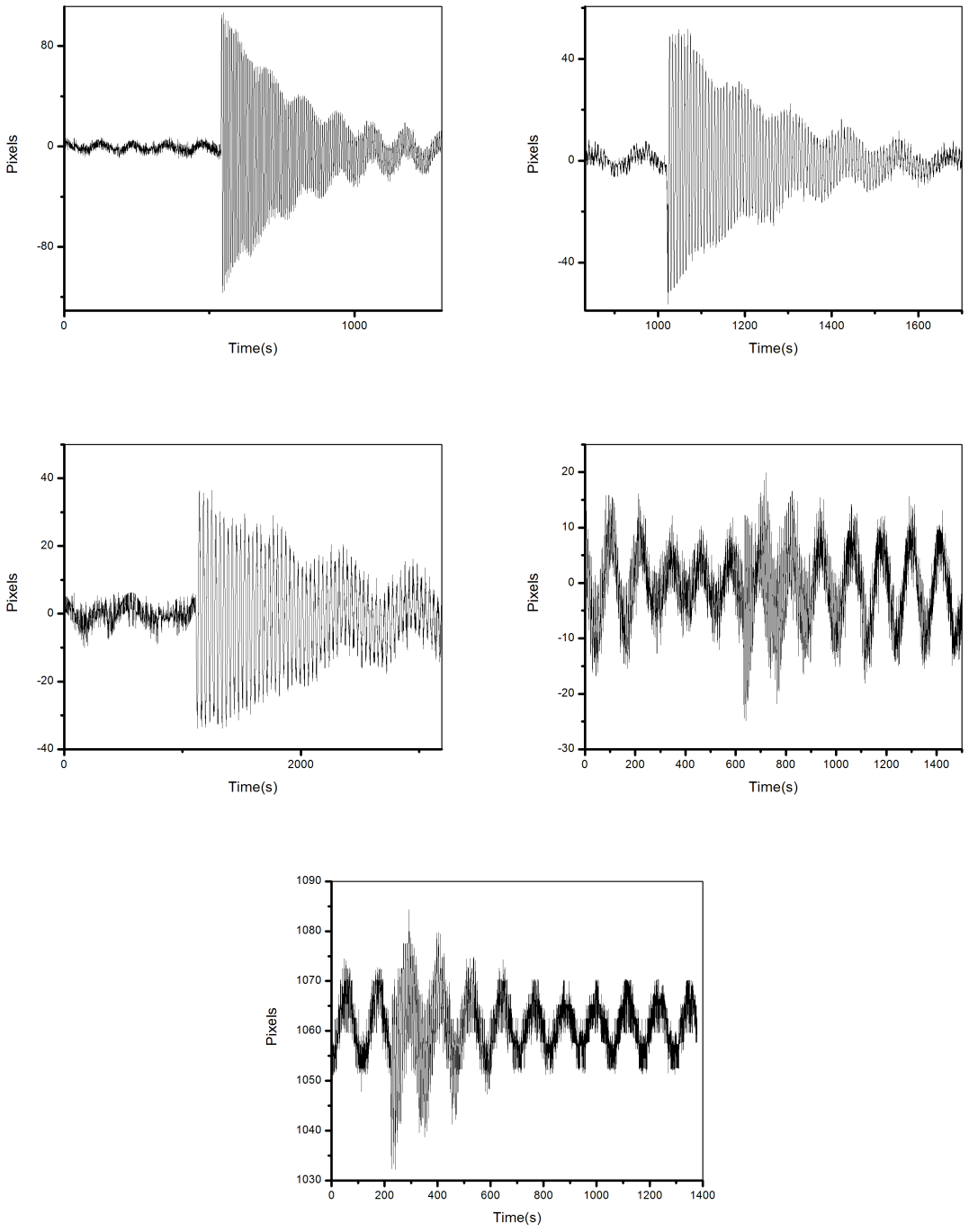

Figure 3.7: The plots show the movement of the reflected point along the horizontal axis on a 3 s exposure of laser light of incident power 2, 1, 0.7, 0.5 and 0.3 mW, respectively.

3.3.3 Noise Filter

Seismic noise is a generic name for a relatively persistent vibration of the ground, due to a multitude of causes, that is a non-interpretable or unwanted component of signals. Seismic noise is a nuisance for activities that are sensitive to vibrations. Those low frequency signals act like an envelope for the oscillations corresponding to the natural time period of the torsion oscillator. Hence, we analyse the data obtained in Fig 3.7 using the following algorithm.

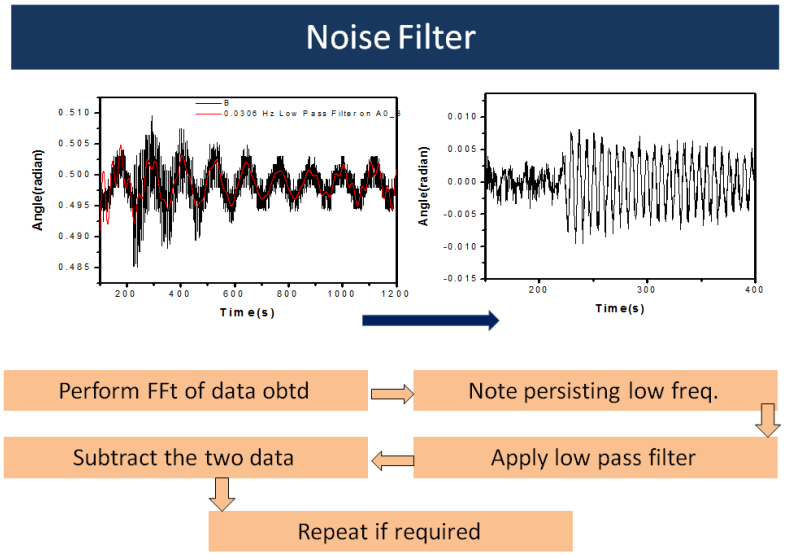

Figure 3.8: Noise Filter Algorithm used for Signal Analysis.

By performing the FFT, as in Section 3.2, we apply a low pass filter corresponding to the pronounced low frequencies persisting in the data. The low pass signal is subtracted from the actual signal and we obtain oscillations of natural time period of the torsion oscillator. This process can be repeated and that acts as a second level of noise filter.The above mentioned processing is done for all the data obtained from 10 mW to 0.3 mW [Fig3.7].

Using the pulse-probe detection technique, The angular precision is of the order of a few miliradian. We obtained a signal corresponding to the minimum incident power of 0.3 mW. Assuming the mirror to be perfectly reflecting, the minimum force detected is as

$$F = \frac{2P}{c} = 2 \times 10^{-12}\ N.$$

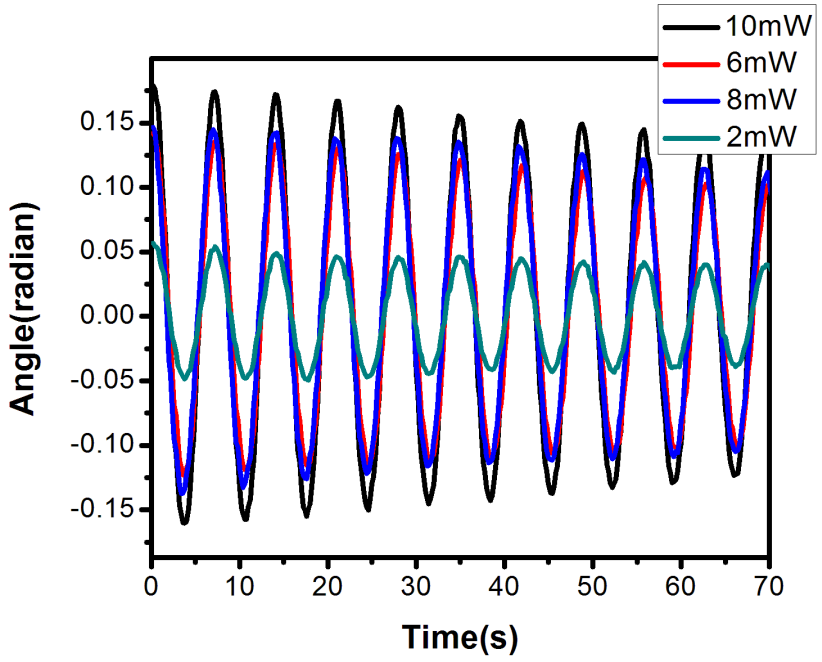

Figure 3.9: Noise filtered signals for high incident pump power from 2-10 mW.

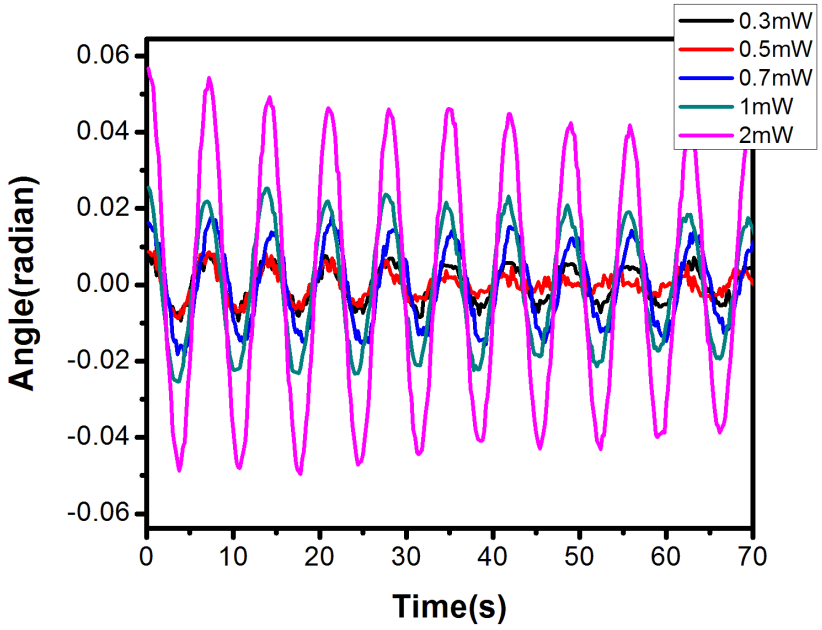

Figure 3.10: Noise filtered signals for incident power from 0.3-2 mW.

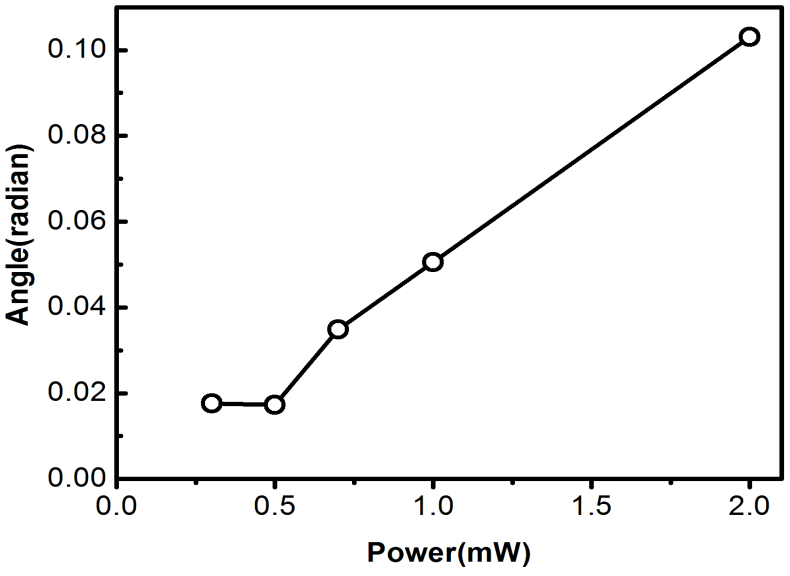

Figure 3.11: Plot of Maximum Angular Deflection with varying incident power.

3.3.4 Correction to Incident Power

Figure 3.12: Plot of Transmitted power (mW) across two glass surfaces vs Incident Power (mW.)

While performing the experiment, we measure the incident power on the glass surface of the chamber. But we cannot assume 100 percent transmittance of pump beam. We measure the change in incident power on the glass surface and then passing through two layers of glass [Fig 3.12]. The transmittance coeffecient 'a' can be calculated as

$$I = \frac{I_0}{a^2}.$$

The average value of 'a' turned out to be 1.19718.

3.3.5 Comparison of Experimental and Theoretical Results

Corrected Incident Power(mW)	Force(x10^{-12})N	Torque(r=1.5mm)(x10^{-15})Nm	Maximum angular deflection(radian)	Torque(Exp)T=κθ (x10^{-15})Nm
0.250588864	1.670592426	2.505888639	0.00878215	5.71129561
0.417648106	2.78432071	4.176481064	0.0087398	5.683754134
0.584707349	3.898048993	5.84707349	0.01808095	11.75858421
0.835296213	5.568641419	8.352962129	0.0257983	16.77740844
1.670592426	11.13728284	16.70592426	0.0518125	33.69522313
5.011777277	33.41184851	50.11777277	0.12905346	83.92733664
6.682369703	44.54913135	6.68E+01	0.141055	91.73229815
8.352962129	55.68641419	83.52962129	0.16733	108.8197189

Figure 3.13: Calculated values of experimental and theoretical torque.

We now make a simple comparison between the theoretical value of incident power given by 2P/c and the value of power according to the calculated κ and the value of maximum angular deflection obtained experimentally.

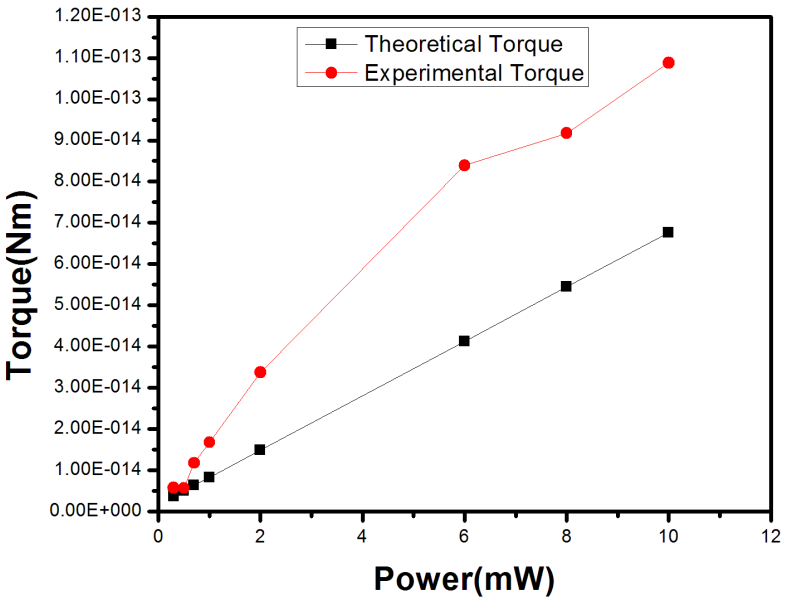

Figure 3.14: Plot of the experimental and theoretical values of torque with varying incident power.

Chapter 4

Conclusions and Future Prospects

- We can surely say that spider silk is a very appropriate material to be used as the torsion wire. It can be easily obtained in very small diameters, has high tensile strength, is durable and lasts well in Ultra High Vacuum conditions. We have obtained threads of diameter of about 300 nm using small baby spiders.
- The pump-probe technique of angle detection tremendously increased the sensitivity of angle measurement but better techniques can be used once we are able to mask the noise level.
- The use of picomotor actuator as the pendulum suspension and using multi-layer vibration isolation for the chamber base and well as suspension mount helped us to go an order of magnitude down for the force detection.
- The lowest force detected has been 2 pN and we could not go beyond as there is a noise background which needs to be worked upon using better vibration Isolation strategies.
- We require even better vibration isolation strategies to exploit the full sensitivity potential. We believe that the improvements listed ahead are in consideration and can be successfully made.
- The experiment will be set in air float conditions over a massive block disconnected from the ground.
- Some way needs to be devised so as to physically isolate the pumping system.
- Mirror Design: Pendulum mass can be designed using materials of very mass and suspended using extremely thin spider silk threads and if such a reflecting material is found, this can improve the sensitivity humongously.
- A better suspension needs to be designed to get rid of the persisting noise. The design needs to be such that once the position of the pendulum is settled, the pendulum can

be disconnected from rotating source. Also, a better design could be using multiple pendulums suspended one over the other[15]. We could also think of an active isolation strategy (feedback) for the pendulum mirror.

- Angle detection techniques with greater precision need to thought about.
- The noise filter algorithm needs to be worked upon for presenting better results.
- Once is a suitable control over the noise level is attained, we might see that under the effect of very small forces what is the dynamics inside the silk thread.

Appendix A

Matlab Program

In this appendix, the Matlab code used for the angle detection of the pendulum in Torsion Pendulum Setup-I has been been presented.

Programs to detect stick in video and Evaluate its Angle

```
videoObject = mmreader('Capture_20160520_5.wmv'); %Upload video file
```

Make directory to save images in current MatLab working folder

```
[s,mess,messid] = mkdir('FramesWithLines');     % Directory would be created
 fid = fopen('Capture_20160520_5', 'w+'); % in current MatLab working folde
```

Input parameters of the Programme

```
numFrames = videoObject.NumberOfFrames;
info = get(videoObject);      % Detailed info about Video file
infoFrameStep = 6;
MaxFrame = 20000; %Max nb of frame to be analysed 194467
NbData = MaxFrame/FrameStep;  % Should be Integer
frmRate = 15.0;               % FrameRate get from info
ThetaCut = 100;               % Cutoff angle for Quadrant jump (0-180)
```

Logic: For each frame get the image snapshot -¿ identify lines -¿ identify angle-¿ open file-¿ save angle-¿ plot angle vs frame corrosponding to stick -¿ plot this line on image -¿ save image

```
Time = zeros(1,MaxFrame/FrameStep);  % PreAllocate Time(:), Angle(:)
Angle = zeros(1,MaxFrame/FrameStep);


m=1; %m counts the frame steps
```

```
for i = 1:FrameStep:MaxFrame; % m counts the frame steps
        % if ( i > 50)
        %      FrameStep = 100
        % end
    rgb = read(videoObject, i);
    gray = rgb2gray(rgb);
    bnw3 = edge(gray,'sobel');

    se90 = strel('line', 3, 90);
    se0 = strel('line', 3, 0);
    BWsdil = imdilate(bnw3, [se90 se0]);
     %figure, imshow(BWsdil)
     BWdfill = imfill(BWsdil, 'holes');
      erodedBW1 = imerode(BWdfill,se0);
      erodedBW2 = imerode(erodedBW1,se0);
      erodedBW3 = imerode(erodedBW2,se0);
      erodedBW4 = imerode(erodedBW3,se0);
      erodedBW5 = imerode(erodedBW4,se0);
      %erodedBW6 = imerode(erodedBW5,se0);
      %figure, imshow(BWdfill);

     [H,theta,rho] = hough(BWdfill);    % Hough Transform to detect Line
     P = houghpeaks(H,8,'threshold',ceil(1.0*max(H(:))));
     lines = houghlines(BWdfill,theta,rho,P,'FillGap',5,'MinLength',20);

     % plot lines on the Original image
     h = figure;
     imshow(rgb), hold on

     max_len = 0;

     for k = 1:length(lines)
         xy = [lines(k).point1; lines(k).point2];
         %determining angle of line w.r.t Yaxis
         % z=[lines(k).theta];
         % Determine the length of line segment under consideration
         len = norm(lines(k).point1 - lines(k).point2);
         plot(xy(:,1),xy(:,2),'LineWidth',1,'Color','green');
```

```
    % Plot beginnings and ends of lines
     plot(xy(1,1),xy(1,2),'x','LineWidth',6,'Color','green');
     plot(xy(2,1),xy(2,2),'x','LineWidth',6,'Color','red');

      if ( len > max_len)
          max_len = len;
          xy_long = xy;
          % determining angle of line w.r.t Xaxis
          %angle=atan2(xy(2,2)-xy(1,2),xy(2,1)-xy(1,1))*180/pi;
          delY = (xy(2,2)-xy(1,2));  % xy(:,1)=x, xy(:,2)=y
          delX = (xy(2,1)-xy(1,1));
            angle = atan(delY/delX)*180/pi;   %Angle value  ??
          % save angle in txt file
          % fprintf(fid, '%1.3f, %1.3f \n', i,angle);

          % write angle on frame
          text(xy(1,1),xy(1,2), [sprintf('%1.3f',angle),'{\circ}'],...
          'Color','y','FontSize',14,'FontWeight','bold');

         % write theta value on frame
         % text(xy(1,2),xy(2,2), [sprintf('%1.3f',z),'{\circ}'],...
         % 'Color','y','FontSize',14,'FontWeight','bold');
      end
end %end of k=1:length(lines)

 frameWithLine = getframe(h);
 [imWithLine,Map] = frame2im(frameWithLine);
 i1 = i;
% getFile name with proper initials
 i1 = int2str(i1);
 if (length(i1) == 1)
    i1 = strcat ('0000', i1);
 end
 if (length(i) == 2)
    i1 = strcat ('000', i1);
 end
 if (length(i1) == 3)
    i1 = strcat ('00', i1);
end
```

```
    if (length(i1) == 4)
        i1 = strcat ('0', i1);
    end
    currentFilename = strcat('FramesWithLines\Frame_', i1 ,'.tif');
    %imwrite(imWithLine, currentFilename);
    close;
```

Angle vs Frame plot in each iteration Loop Not scaled

```
    Time(m) = m-1;  % integers t = (m-1)*FrameStep/FrameRate : t=0 set for 1st f
    Angle(m) = angle;

    plot(Time(:), Angle(:), '--rs','LineWidth',1)
    xlabel('frame count'), ylabel('angle(deg)'), title('angle vs frame');

   m = m+1;
end

 Time = zeros(1,MaxFrame/FrameStep);  % PreAllocate Time(:), Angle(:)
 Angle = zeros(1,MaxFrame/FrameStep);


  m=1; %m counts the frame steps
for i = 1:FrameStep:MaxFrame; % m counts the frame steps
       % if ( i > 50)
       %     FrameStep = 100
       % end
   rgb = read(videoObject, i);
   gray = rgb2gray(rgb);
   bnw3 = edge(gray,'sobel');

   se90 = strel('line', 3, 90);
   se0 = strel('line', 3, 0);
   BWsdil = imdilate(bnw3, [se90 se0]);
    %figure, imshow(BWsdil)
    BWdfill = imfill(BWsdil, 'holes');
     erodedBW1 = imerode(BWdfill,se0);
     erodedBW2 = imerode(erodedBW1,se0);
     erodedBW3 = imerode(erodedBW2,se0);
     erodedBW4 = imerode(erodedBW3,se0);
```

```
 erodedBW5 = imerode(erodedBW4,se0);
 %erodedBW6 = imerode(erodedBW5,se0);
 %figure, imshow(BWdfill);

[H,theta,rho] = hough(BWdfill);   % Hough Transform to detect Line
P = houghpeaks(H,8,'threshold',ceil(1.0*max(H(:))));
lines = houghlines(BWdfill,theta,rho,P,'FillGap',5,'MinLength',20);

% plot lines on the Original image
h = figure;
imshow(rgb), hold on

max_len = 0;

for k = 1:length(lines)
    xy = [lines(k).point1; lines(k).point2];
    %determining angle of line w.r.t Yaxis
    % z=[lines(k).theta];
    % Determine the length of line segment under consideration
    len = norm(lines(k).point1 - lines(k).point2);
    plot(xy(:,1),xy(:,2),'LineWidth',1,'Color','green');

    % Plot beginnings and ends of lines
    plot(xy(1,1),xy(1,2),'x','LineWidth',6,'Color','green');
    plot(xy(2,1),xy(2,2),'x','LineWidth',6,'Color','red');

     if ( len > max_len)
         max_len = len;
         xy_long = xy;
         % determining angle of line w.r.t Xaxis
         %angle=atan2(xy(2,2)-xy(1,2),xy(2,1)-xy(1,1))*180/pi;
         delY = (xy(2,2)-xy(1,2));  % xy(:,1)=x, xy(:,2)=y
         delX = (xy(2,1)-xy(1,1));
           angle = atan(delY/delX)*180/pi;   %Angle value  ??
         % save angle in txt file
         % fprintf(fid, '%1.3f, %1.3f \n', i,angle);

         % write angle on frame
         text(xy(1,1),xy(1,2), [sprintf('%1.3f',angle),'{\circ}'],...
```

```
            'Color','y','FontSize',14,'FontWeight','bold');

            % write theta value on frame
            % text(xy(1,2),xy(2,2), [sprintf('%1.3f',z),'{\circ}'],...
            % 'Color','y','FontSize',14,'FontWeight','bold');
        end
    end %end of k=1:length(lines)

    frameWithLine = getframe(h);
    [imWithLine,Map] = frame2im(frameWithLine);
    i1 = i;
    % getFile name with proper initials
    i1 = int2str(i1);
    if (length(i1) == 1)
       i1 = strcat ('0000', i1);
    end
    if (length(i) == 2)
       i1 = strcat ('000', i1);
    end
    if (length(i1) == 3)
       i1 = strcat ('00', i1);
    end
    if (length(i1) == 4)
       i1 = strcat ('0', i1);
    end
    currentFilename = strcat('FramesWithLines\Frame_', i1 ,'.tif');
    %imwrite(imWithLine, currentFilename);
    close;
```

Angle vs Frame plot in each iteration Loop Not scaled

```
    Time(m) = m-1;  % integers t = (m-1)*FrameStep/FrameRate : t=0 set for 1st f
    Angle(m) = angle;

    plot(Time(:), Angle(:), '--rs','LineWidth',1)
    xlabel('frame count'), ylabel('angle(deg)'), title('angle vs frame');

   m = m+1;
end

\noindent\textbf{Shifthing data for smoothing Quadrant jumps}
```

```
\begin{lstlisting}
  for m=1:1:NbData  % NbData = MaxFrame/FrameStep
   if (m>1);
        if ((Angle(m)- Angle(m-1)) > ThetaCut);
           Angle(m:NbData) = Angle(m:NbData) - 180;
        elseif ((Angle(m)- Angle(m-1)) < - ThetaCut);
           Angle(m:NbData) = Angle(m:NbData) + 180;
        end
    end
  end
  Time(:) = Time(:)*(FrameStep/frmRate);  % Frame to Second scaling
 for m=1:1:NbData  % Save data in file
 fprintf(fid, '%1.3f, %1.3f \n', Time(m),Angle(m));
 end


plot(Time(:), Angle(:), '.','LineWidth',4)
xlabel('Time (s)'), ylabel('Angle(deg)'), title('Angle(deg) vs Time(s)');
```

Appendix B

Vacuum Chamber Design

In this appendix, the detailed design and component details of the Ultra High Vacuum Chamber used for silk torsion pendulum suspension has been presented.

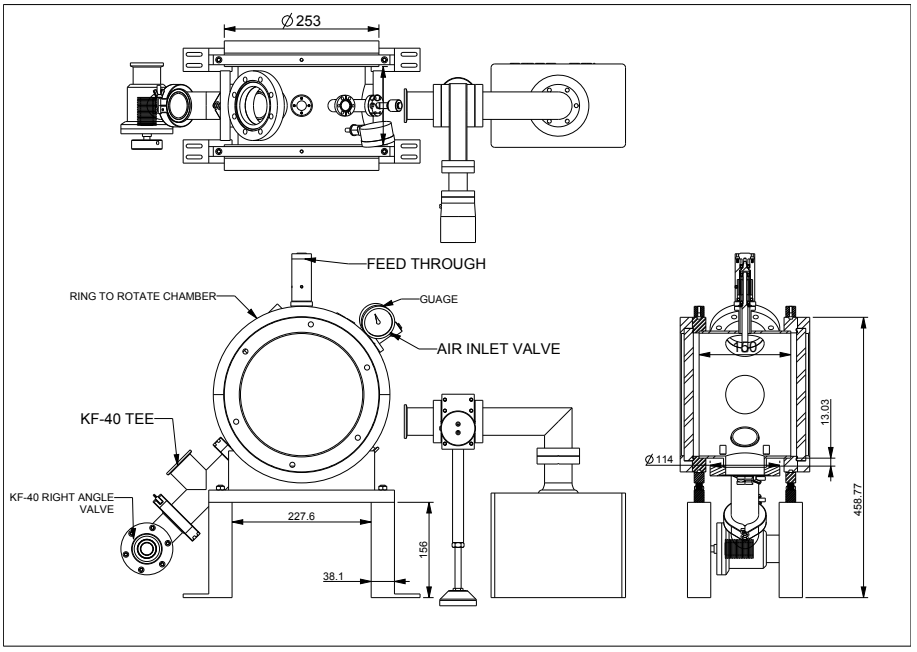

Figure B.1: Design of the UHV Chamber used for torsion pendulum suspension.

Bibliography

[1] F Mueller, S Heugel, and LJ Wang. Femto-newton light force measurement at the thermal noise limit. *Optics letters*, 33(6):539–541, 2008.

[2] Nader Jalili and Karthik Laxminarayana. A review of atomic force microscopy imaging systems: application to molecular metrology and biological sciences. *Mechatronics*, 14(8):907–945, 2004.

[3] Vladimir Borisovich Braginsky and Anatoliĭ Manukin. Measurement of weak forces in physics experiments.

[4] C Zensen, N Villadsen, F Winterer, SR Keiding, and T Lohmüller. Pushing nanoparticles with light—a femtonewton resolved measurement of optical scattering forces. *Apl Photonics*, 1(2):026102, 2016.

[5] Constanze Höhberger Metzger and Khaled Karrai. Cavity cooling of a microlever. *Nature*, 432(7020):1002–1005, 2004.

[6] F Mueller, S Heugel, and LJ Wang. Subkelvin cooling of a gram-sized oscillator. *Applied Physics Letters*, 92(4):044101, 2008.

[7] Scott Yantek. Precision tilt measurements for a cryogenic torsion balance.

[8] Henry Cavendish. Experiments to determine the density of the earth. by henry cavendish, esq. frs and as. *Philosophical Transactions of the Royal Society of London*, 88:469–526, 1798.

[9] Ernest Fox Nichols and Gordon Ferrie Hull. The pressure due to radiation. 38(20):559–599, 1903.

[10] F Mueller, S Heugel, and LJ Wang. Observation of optomechanical multistability in a high-q torsion balance oscillator. *Physical Review A*, 77(3):031802, 2008.

[11] F Mueller, S Heugel, and LJ Wang. Optomechanical stochastic resonance in a macroscopic torsion oscillator. *Physical Review A*, 79(3):031804, 2009.

[12] Philip Ball. Focus: Detecting femtonewton forces in water. *Physics*, 9:61, 2016.

[13] Lin Römer and Thomas Scheibel. The elaborate structure of spider silk. *Prion*, 2(4):154–161, 2008.

[14] R Abbott, R Adhikari, G Allen, S Cowley, E Daw, D DeBra, J Giaime, G Hammond, M Hammond, C Hardham, et al. Seismic isolation for advanced ligo. *Classical and Quantum Gravity*, 19(7):1591, 2002.

[15] NA Robertson, G Cagnoli, DRM Crooks, E Elliffe, JE Faller, P Fritschel, Stefan Goßler, A Grant, A Heptonstall, J Hough, et al. Quadruple suspension design for advanced ligo. *Classical and Quantum Gravity*, 19(15):4043, 2002.

[16] Lulu Liu, Simon Kheifets, Vincent Ginis, and Federico Capasso. Subfemtonewton force spectroscopy at the thermal limit in liquids. *Physical Review Letters*, 116(22):228001, 2016.

[17] Hasok Chang. Electrolysis: Piles of confusion and poles of attraction. In *Is Water H2O?*, pages 71–131. Springer, 2012.

[18] AB Matsko, EA Zubova, and SP Vyatchanin. The value of the force of radiative friction. *Optics communications*, 131(1):107–113, 1996.